

# 1 Spatio-temporal domains of wildfire-prone teleconnection patterns in the Western 2 Mediterranean Basin

3 Marcos Rodrigues<sup>1,2,9</sup>, Michela Mariani<sup>3</sup>, Ana Russo<sup>4</sup>, Michele Salis<sup>5</sup>, Luiz Galizia<sup>6</sup>, Adrian  
4 Cardil<sup>2,7,8</sup>

5 <sup>1</sup> Department of Agricultural and Forest Engineering, University of Lleida, E-25198 Lleida,  
6 Spain

7 <sup>2</sup> Joint Research Unit CTFC – AGROTECNIO, E-25280 Solsona, Spain

8 <sup>3</sup> School of Geography, University of Nottingham, Nottingham, NG72RD, United Kingdom

9 <sup>4</sup> Instituto Dom Luiz (IDL), Faculdade de Ciências da Universidade de Lisboa, 1749 – 016  
10 Lisboa, Portugal

11 <sup>5</sup> National Research Council, Institute of BioEconomy (CNR-IBE), Traversa La Crucca 3, 07100,  
12 Sassari, Italy

13 <sup>6</sup> INRAE, RECOVER, Aix-Marseille Univ., Aix-en-Provence, France

14 <sup>7</sup> Department of Crop and Forest Sciences, University of Lleida, E-25198 Lleida, Spain

15 <sup>8</sup> Technosylva Inc., La Jolla, CA, USA

16 <sup>9</sup> GEOFOREST Group, Department of Geography and Land Management, University of  
17 Zaragoza, Spain

18 Corresponding author: Marcos Rodrigues ([marcos.rodrigues@udl.cat](mailto:marcos.rodrigues@udl.cat))

## 19 Key Points:

- 20 • We found three distinctive but homogenous domains of influence of climate  
21 teleconnections patterns.
- 22 • The SCAND pattern exerts a zonal influence over the western Mediterranean basin. NAO  
23 controls the IP and WeMOi the Mediterranean coast.
- 24 • Positive moisture winter-spring anomalies coupled to short-term dry and warm conditions  
25 boost most of the wildfire activity.  
26

## 27 **Plain language summary**

28 We synthesized the climate influence on wildfire activity over the Western Mediterranean Basin  
29 into three distinctive configurations. We applied computer-assisted statistical analysis on  
30 historical fire records from national/regional agencies and climate-related data (the so-called  
31 climate teleconnection indexes; e.g. 'El Niño' or the NAO). Burned area size over the entire basin  
32 tends to be larger under the confluence of rainy winter-spring and sudden heat waves and dry  
33 spells during summer, which is governed by the Scandinavian pattern. In the Mediterranean  
34 coast of Spain fires occur more frequently under sustained calm and warm conditions while they  
35 grow larger when winds blow from the western side of the Iberian Peninsula. These conditions  
36 depend on the North Atlantic Oscillation and Western Mediterranean Oscillation pattern  
37 (WeMOi), respectively. Fire activity in Southern France, Corsica and Sardinia seems to be linked  
38 to the lack of rainfall, which is regulated by the atmospheric conditions over the Mediterranean  
39 sea, mostly controlled by the WeMOI pattern.

## 40 **Abstract**

41 This work explores the main climate teleconnections influencing the Western Mediterranean  
42 Basin to outline homogeneous fire-prone weather domains combining cross-correlation time  
43 series and cluster analysis. We found a zonal effect of the Scandinavian pattern over the entire  
44 region with an interesting alternation of phases from positive during winter-spring (increased  
45 rainfall leading to fuel accumulation) to negative (dry conditions) modes during summer  
46 controlling burned area and fire size. The NAO dominates the number of fires over the Iberian  
47 Peninsula (IP) while the Western Mediterranean Oscillation pattern modulates fire activity over  
48 the Mediterranean coast in the IP (linked to westerly winds), Southern France, Corsica and  
49 Sardinia (rainfall regulation). These distinctive influence traits resulted in 3 different domains  
50 splitting the IP into a Mediterranean rim along the coast (from southern Spain to southwestern  
51 France) and an inland and western region (Portugal plus western Spain); and a third in  
52 southeastern France, Corsica and Sardinia.

## 53 **1 Introduction**

54 Wildfires are a key ecosystem process that modulates vegetation distribution and  
55 evolution (Bond, Woodward and Midgley, 2005) and impacts the global carbon cycle (Jones et  
56 al., 2019), whilst having substantial economic and social impacts (Moritz et al., 2014). During  
57 the last two decades, most of the extreme wildfires reported as being economically or socially  
58 catastrophic were concentrated in suburban areas intermixed with flammable forests, particularly  
59 in the western United States (Radeloff et al., 2018), southeastern Australia (Bowman et al., 2017)  
60 and the Mediterranean Basin (Modugno et al., 2016). The latter was specifically identified as a  
61 disaster-prone landscape with projections suggesting an increase of extreme fire weather of 50-  
62 100% by the end of the current century (Bowman et al., 2017). Currently, most of the total  
63 burned area in Europe occurs in this region during the summer, with an average of about 4,500  
64 km<sup>2</sup>/yr, an area that is expected to increase (Ganteaume et al., 2013; Turco et al., 2017).

65 Mediterranean Europe occupies a climatic transitional area under the alternate influence  
66 of sub-tropical and temperate climates (Lionello, 2012). In this area, ecosystems and human  
67 populations are affected by frequent weather-driven natural hazards, such as droughts (Hoerling  
68 et al., 2012; Russo et al., 2017), heat waves (Sánchez-Benítez et al., 2018; Sousa et al., 2019) and  
69 wildfires (Ruffault et al., 2020). The frequency and severity of these extreme weather-driven

70 events are likely to increase under climate change (Dupuy et al., 2020; Lionello and Scarascia,  
71 2020). Additionally, the compound occurrence of drought and heatwave events has recently  
72 increased (Vogel et al., 2021), a trend that will persist according to future forecasts (Zscheischler  
73 et al., 2018; AghaKouchak et al., 2020). Additionally, the summer fire activity in Mediterranean-  
74 type ecosystems is thought to be sensitive to antecedent winter rainfall pulses that could lead to  
75 an accumulation of fuels, while concurrent droughts and/or hot-dry winds are the short-term  
76 driver of wildfires (Moritz et al., 2012). Predicting future fire activity does not only hinge on  
77 understanding the short-term fire weather patterns, but also the longer-term of climate variability  
78 (Rodrigues et al., 2020; Vieira et al., 2020), particularly on biomass accumulation mediated by  
79 regional-scale drivers (Moritz et al., 2012).

80 Previous studies suggest that coincident drought conditions and high temperatures  
81 promote large wildfires across southern Europe (Camiá et al., 2009; Bedia et al., 2013; Urbieto et  
82 al., 2015; Gouveia et al., 2016). Nevertheless, the role of antecedent large-scale climate  
83 conditions remains a debated topic across much of the Mediterranean Europe. Previous analyses  
84 of the linkages between fire activity and meteorological variables in southern France (Ruffault et  
85 al., 2016), Greece (Koutsias et al., 2013; Gouveia et al., 2016) and the Iberian Peninsula (Turco  
86 et al., 2013; Vieira, Russo and Trigo, 2020) reveal significant correlations with both same-  
87 summer and lagged climate variables.

88 Climate teleconnections (CTs) have a synchronous influence on weather at a regional  
89 scale (sub-continental) while playing a key role in modulating temperature and precipitation  
90 patterns at both interannual and decadal scales (e.g., Ascoli et al., 2017; Harris and Lucas,  
91 2019). These patterns can subsequently dictate plant growth (fuel amount) and its dryness, and  
92 hence modulate the occurrence and spread of wildfires (Cai et al., 2014; Mariani, Veblen and  
93 Williamson, 2018). CTs patterns are expected to become more extreme in the future (Power et  
94 al., 2013; Cai et al., 2014), potentially exacerbating their effects on wildfires (Mariani et al.,  
95 2018). Thus, the links between CTs and fire activity have been investigated in various regions  
96 (Kitzberger et al., 2007; Mariani, et al., 2018; Cardil et al., 2021; Rodrigues et al., 2021).  
97 However, the role of large-scale CTs on wildfire occurrence and spread has not yet been fully  
98 explored in the western Mediterranean region (Royé et al., 2020). Within this area, various CTs  
99 influence weather, including the North Atlantic Oscillation (NAO), the East Atlantic (EA), the  
100 Atlantic Multidecadal Oscillation (AMO), the El Niño Southern Oscillation (ENSO), the  
101 Mediterranean Oscillation (MOI), the Pacific Decadal Oscillation (PDO), the Scandinavian  
102 pattern (SCAND) and the Western Mediterranean oscillation (WeMOi). In a recent study carried  
103 out in the Iberian Peninsula, fire danger patterns were found to be significantly correlated to the  
104 WeMOi, MOI, NAO, ENSO and SCAND indexes (Rodrigues et al., 2021).

105 Investigating mechanisms behind climate-fire dynamics, including lagged relationships  
106 between climatic conditions and wildfire activity (i.e., fuel built-up fostered by above average  
107 antecedent moist conditions), is critical for understanding the future of Mediterranean  
108 ecosystems. Despite the clear importance of wildfires in shaping vegetation and impacting  
109 human lives under the projected climate change (Moritz et al., 2012; Bowman et al., 2017), the  
110 climatic drivers of fire activity through time remain poorly understood in many regions on Earth,  
111 including the European Mediterranean Basin (Turco et al., 2017). In this paper, we provide a  
112 new assessment of the climatic drivers of wildfire occurrence and spread within the western  
113 Mediterranean region over the period 1980-2015. We expand the spatial and temporal scales of  
114 work carried out so far in the Iberian Peninsula (IP) on the links between wildfires and CTs,

115 while focusing on actual fire features (namely number of ignitions, burned area and fire size)  
116 rather than fire-weather indexes (Rodrigues et al., 2021). The main goal of the present work is  
117 assessing spatio-temporal climate domains reflecting the interaction of climate teleconnections  
118 and their potential influence in wildfire activity across western Mediterranean Europe. We aim to  
119 address the following research questions: 1) Which are the leading CTs over wildfire occurrence  
120 and spread across western Mediterranean Europe?; 2) Can we identify transboundary domains of  
121 CT influence?; and 3) Is biomass limitation generating a lagged relationship between CTs and  
122 wildfires? Answering these questions will provide a better understanding of the regional climate-  
123 fire linkages, which would allow a better preparation for potential future wildfires or prompt  
124 timely fuel load reduction programmes.

## 125 **2 Materials and Methods**

126 We calculated the Pearson's R correlation coefficient between monthly time series of fire  
127 features (number of fires, burned area and fire size) and CTs in each grid cell. Thus we retrieved  
128 a set of Pearson correlation coefficients for each combination of fire feature, CT and lag (0, 3, 6  
129 and 9 months) for each grid cell. The spatial pattern of correlations was summarized in maps  
130 depicting the direction (either positive or negative) and the significance ( $p < 0.05$ ,  $R = \pm 0.34$ ) of the  
131 association.

132 To outline potential climatic domains resulting from the interaction of CT at multiple  
133 time scales we submitted the correlation coefficients to a cluster analysis. Identifying such  
134 domains will enable us to better understand the climatic forcing of wildfire activity. Our  
135 approach is heavily focused on identifying transnational climatic regions under the premise that  
136 homogenous patterns of both wildfire activity and climate factors do exist. We adopted a  
137 hierarchical cluster approach using *Euclidean Distance* as dissimilarity measure and *ward.D2* as  
138 agglomeration criterion, which aims to create groups such that variance is minimized within  
139 them. Clusters were trained for each fire feature separately and the optimal number of clusters  
140 (i.e., climate domains) was determined from the set of criteria available in the *nbClust* package  
141 (Charrad et al., 2014). Climate domains were then characterized according to the observed  
142 distribution of CT correlation, indicating the most influential patterns in terms of significance  
143 and direction of the relationship.

## 144 **3 Data**

### 145 **3.1 Study region and fire data**

146 The region under study extends over the Western Mediterranean Basin, including  
147 Portugal, Spain, Southern France, Corsica and Sardinia (Italy), which are among the most fire-  
148 affected region of Europe. Fire data were obtained from the national/regional wildfire databases  
149 of Portugal (ICNF, <http://www2.icnf.pt/portal/florestas/dfci/inc/estat-sgif>), Spain (EGIF;  
150 [https://www.miteco.gob.es/es/biodiversidad/servicios/banco-datos-naturaleza/informacion-  
151 disponible/incendios-forestales.aspx](https://www.miteco.gob.es/es/biodiversidad/servicios/banco-datos-naturaleza/informacion-disponible/incendios-forestales.aspx)), France (Prométhée;  
152 <https://www.promethee.com/incendies>) and Sardinia (CFVA;  
153 [http://www.sardegnaeoportale.it/webgis2/sardegnamappe/?map=aree\\_tutelate](http://www.sardegnaeoportale.it/webgis2/sardegnamappe/?map=aree_tutelate)). We retrieved  
154 all fire records in the period 1980-2015, retaining only those larger than 100 ha to prevent  
155 inhomogeneities related to fire detection and compilation. For each fire record we extracted the  
156 date and place of ignition and the final size. Fire events were aggregated into a regular grid of  
157  $0.5^\circ$  resolution to prevent undesired effects due to partial/inaccurate location information. For

158 each cell, we calculated the burned area, the total number of fires and the 95th percentile of fire  
 159 size on a monthly basis. Fire features were aggregated as the sum of the number of fires and  
 160 burned areas, and the 95th percentile of fire size, in the period May-to-October. Finally, we  
 161 applied an unweighted moving window procedure using a bandwidth of 500 km. This procedure  
 162 helps smoothing the spatial distribution of fire activity to facilitate the identification of spatial  
 163 patterns of association with large-scale climate teleconnections (Koutsias et al., 2016; Andela et  
 164 al., 2017). Because of the unweighted moving window, a given pixel does not represent its actual  
 165 location but rather the 500km region surrounding it, increasing the average number of fire events  
 166 per pixel to sufficient amount (from 0.07 to 18.16) for the investigation of extremes.

### 167 3.2 Climate teleconnection patterns

168 We investigated seven CT patterns, known to be among the most influential factors  
 169 modulating wildfires in the Western Mediterranean Basin:

170 - The NAO computed as the Gibraltar- Reykjavik normalized Sea Level Pressure (Jones,  
 171 Jonsson and Wheeler, 1997); <https://crudata.uea.ac.uk/cru/data/nao/nao.dat>.

172 - The EA teleconnection pattern index, which is structurally similar to the NAO, and  
 173 consists of a north-south dipole of anomaly centers spanning the North Atlantic from east to west  
 174 (Barnston and Livezey, 1987); <http://www.cpc.ncep.noaa.gov/data/teledoc/ea.shtml>.

175 - The SCAND, which consists of a primary circulation center over Scandinavia, with  
 176 weaker centers of opposite sign over western Europe and eastern Russia/ western Mongolia, and  
 177 known there as Eurasia-1 (Barnston and Livezey,  
 178 1987); <https://www.cpc.ncep.noaa.gov/data/teledoc/scand.shtml>.

179 - The ENSO, which was calculated from the HadISST1. It is the area averaged sea surface  
 180 temperature (SST) from 5S-5N and 170-120W (Rayner et al., 2003);  
 181 [https://psl.noaa.gov/gcos\\_wgsp/Timeseries/Nino34/](https://psl.noaa.gov/gcos_wgsp/Timeseries/Nino34/).

182 - The PDO, which was derived as the leading PC of monthly SST anomalies in the North  
 183 Pacific Ocean, poleward of 20N (Mantua et al., 1997);  
 184 <https://psl.noaa.gov/data/climateindices/list/>.

185 - The MOI, defined by Conte, Giuffrida and Tedesco (1989) as the normalized pressure  
 186 difference between Algiers and Cairo; <https://crudata.uea.ac.uk/cru/data/moi/moi1.output.dat>.

187 The WeMOi, which is an index measuring the difference between the standardized  
 188 atmospheric pressure recorded at Padua in northern Italy, and San Fernando, Cádiz in  
 189 Southwestern Spain (Martin-Vide and Lopez-Bustins, 2006);  
 190 [http://www.ub.edu/gc/documents/Web\\_WeMOi-2020.txt](http://www.ub.edu/gc/documents/Web_WeMOi-2020.txt).

191 CTs were averaged into the corresponding 6-month time frame. In addition to  
 192 synchronous correlation (i.e., lag =0 May-to-October), we investigated asynchronous effects in  
 193 the CTs signal by exploring a lag of 3 (February-July), 6 (November-May) and 9 (September-  
 194 February) months before the summertime.

## 195 **4 Results**

### 196 4.1 Influence of climate teleconnections on fire features

197 The spatial patterns of correlation between CTs and the selected fire features (burned  
198 area, number of fires and fire size) depicted varied spatial arrangements. It should also be  
199 highlighted that the statistical significance was non-stationary over space and differed among  
200 CTs (Figure 1, 2 and 3). The CT indices depicting the strongest positive or negative correlations  
201 were SCAND, WeMOI and NAO.

202 The SCAND index showed significant negative synchronous correlations (lag 0) with  
203 burned area almost in the entire study area. Surprisingly, we identified a sharp transition across  
204 the different time lags from positive association at lag 6 (antecedent winter), though statistically  
205 significant only in midland Spain. The NAO index was positively correlated above 40° latitude in  
206 the IP and Southern France at lag 0. NAO also denoted a significant lagged signal (6 and 9  
207 months before summer) in Southern France, Corsica and Sardinia. The WeMOI index is  
208 correlated to increased burned area in Sardinia, Corsica, and the Mediterranean coast of Spain  
209 and France from lag 3 to 9 (Figure 1). The correlations with MOI and PDO were lower than the  
210 aforementioned indices and only significant in specific enclaves (i.e., MOI in the south of  
211 Sardinia at lag 9 and PDO in Spain at lag 9).

212 In terms of correlation results with the number of fires (Figure 2), NAO was clearly the  
213 dominant pattern, being positively correlated in the IP and Southern France at time lag 0 and  
214 Southern France and Sardinia at lag 9. The effect of the SCAND index differed, in spatial terms,  
215 from the burned area analysis. This index was only significant (negatively) in Corsica, the north  
216 of Sardinia, Southern France and NE Spain at lag 0. It was found to be positively correlated in  
217 Sardinia, Southern France and the Spanish Mediterranean coast at lag 3. The contribution of the  
218 persistent positive WeMOI phase (and to a lesser extent PDO) was significantly evident in the  
219 Mediterranean at all lags. The MOI was also significant in Sardinia, Corsica and some coastal  
220 Mediterranean areas of France at lag 6 and 9.

221 The significance of all indices explaining fire size was lower compared to burned area  
222 and fire ignitions (Figure 3). Similarly to the burned area, the SCAND index significantly  
223 explained the size of fires, transitioning as well from positive association in lag 6 to antiphase  
224 correlation at lag 0 in most of the study area. NAO shows significant correlations with fire size in  
225 Sardinia, Southern France and Corsica at lag 3 (antecedent spring) and the WeMOI index  
226 showed a positive correlation along the Spanish Mediterranean coast, though only significant at  
227 lag 3.

228 The other CT modes (EA and ENSO) did not show significant effects anywhere in the  
229 study region.

### 230 4.2 Spatio-temporal domains of climate teleconnections

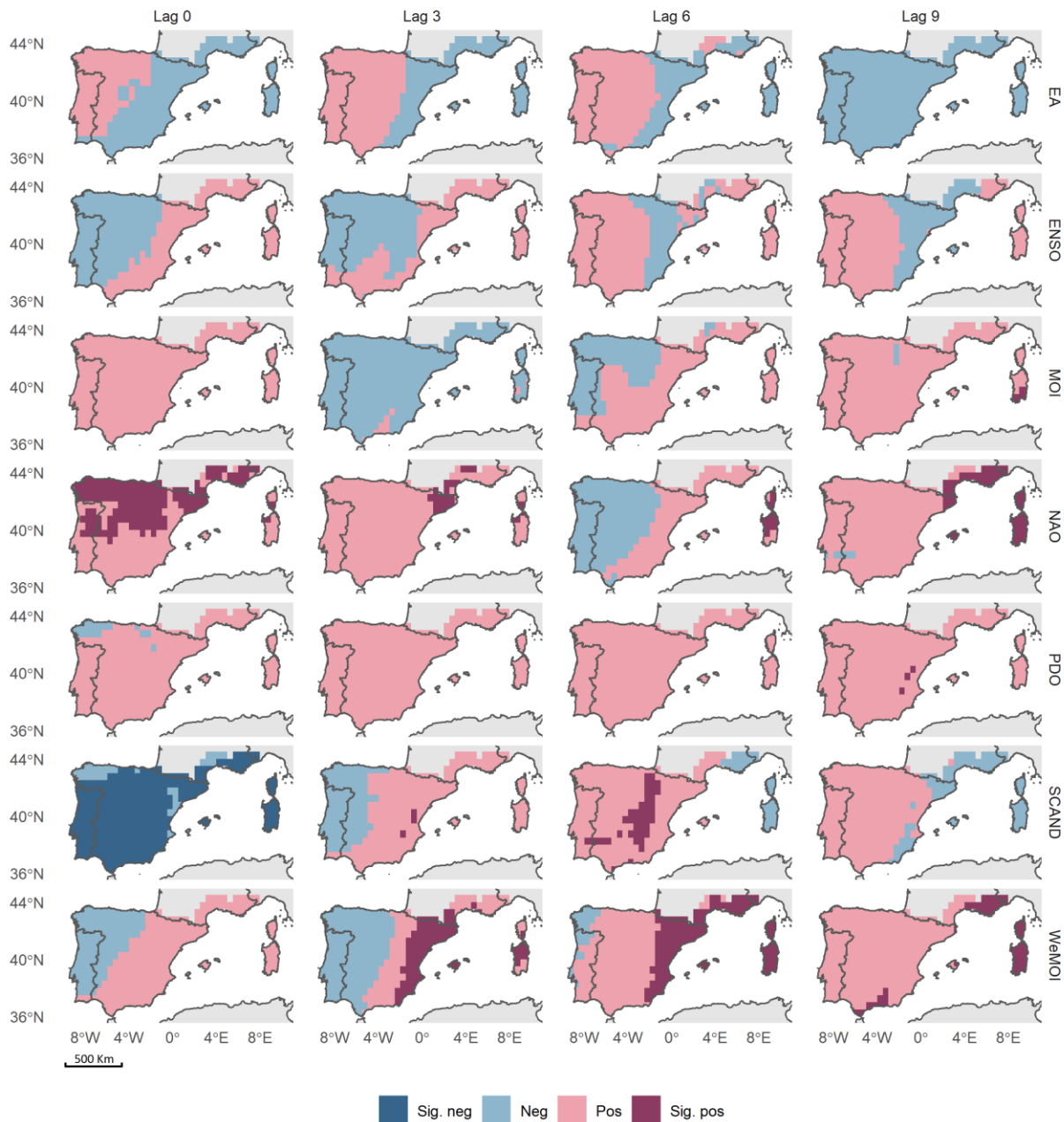
231 We identified three clusters based on most influential CT indices (SCAND, WeMOI and  
232 NAO) that consistently outlined coincident domains among the three fire features considered in  
233 this work (Figure 4). These homogeneous zones reflect the climatic gradient from Atlantic (Zone  
234 1) to Mediterranean conditions (Zones 2 and 3). Despite the geographical concordance of the  
235 patterns, we observed clear differences in the inner contribution of CTs in terms of association

236 and significance of CTs and temporal scales of influence, which significantly varied across fire  
237 features.

238         Zone 1 gathered the influence of SCAND and NAO patterns on all fire features This CT  
239 domain extends over the western IP, excluding the Mediterranean coast. Positive NAO at lag 0  
240 and a sharp transition from positive to negative SCAND (also observed in zones 2 and 3) are the  
241 distinctive traits of the region. Zone 2 seems to act as a transition area from Atlantic to  
242 Mediterranean conditions. It covers the Spanish Mediterranean coast, extending over the western  
243 portion of southern France. The SCAND pattern is still exerting a strong influence, showing  
244 negative and synchronous associations. Zone 2 better relates to positive association with the  
245 WeMOI pattern, which boosts both burned area and fire size but showed weaker influence in fire  
246 ignitions, still strongly linked to synchronic NAO.

247         The third domain (Zone 3), was clearly led by the WeMOI pattern, exerting a strong  
248 positive association with burned area and number of fire ignitions. The influence of WeMOI  
249 extends from lag 9 to 0 in the case of fire ignitions, shortening in the case of burned area (3 to 9).  
250 Again, the SCAND index depicted a synchronous negative influence in the entire study region  
251 and a sharp transition. NAO significantly explained fire features at different time lags: burned  
252 area (lag 0), number of fires (lag 3), fire size (lag 9).

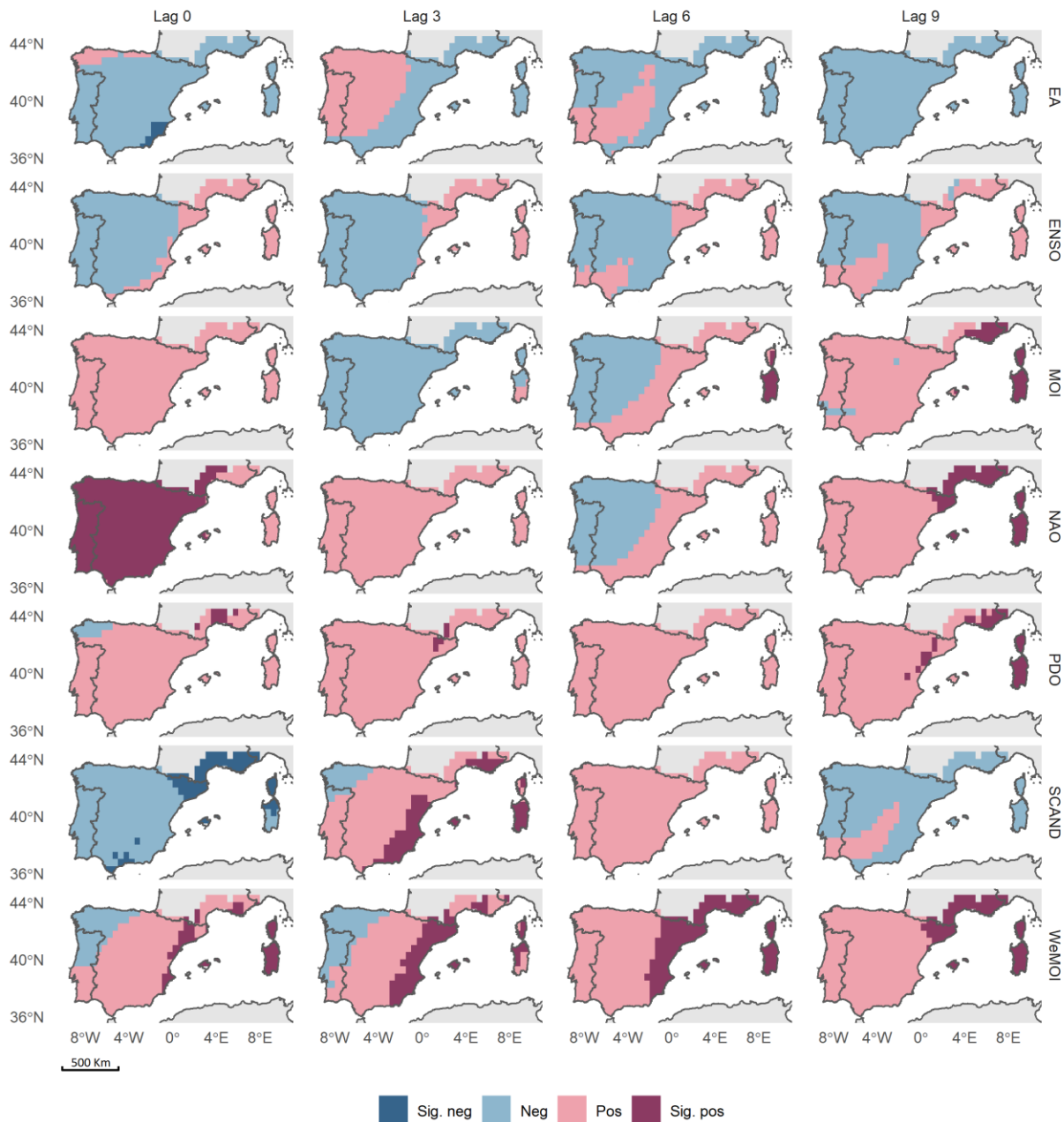
Correlation with burned area during the warm season (May-October)  
 Pearson's R significant ( $p < 0.05$ ) at  $R = 0.34$



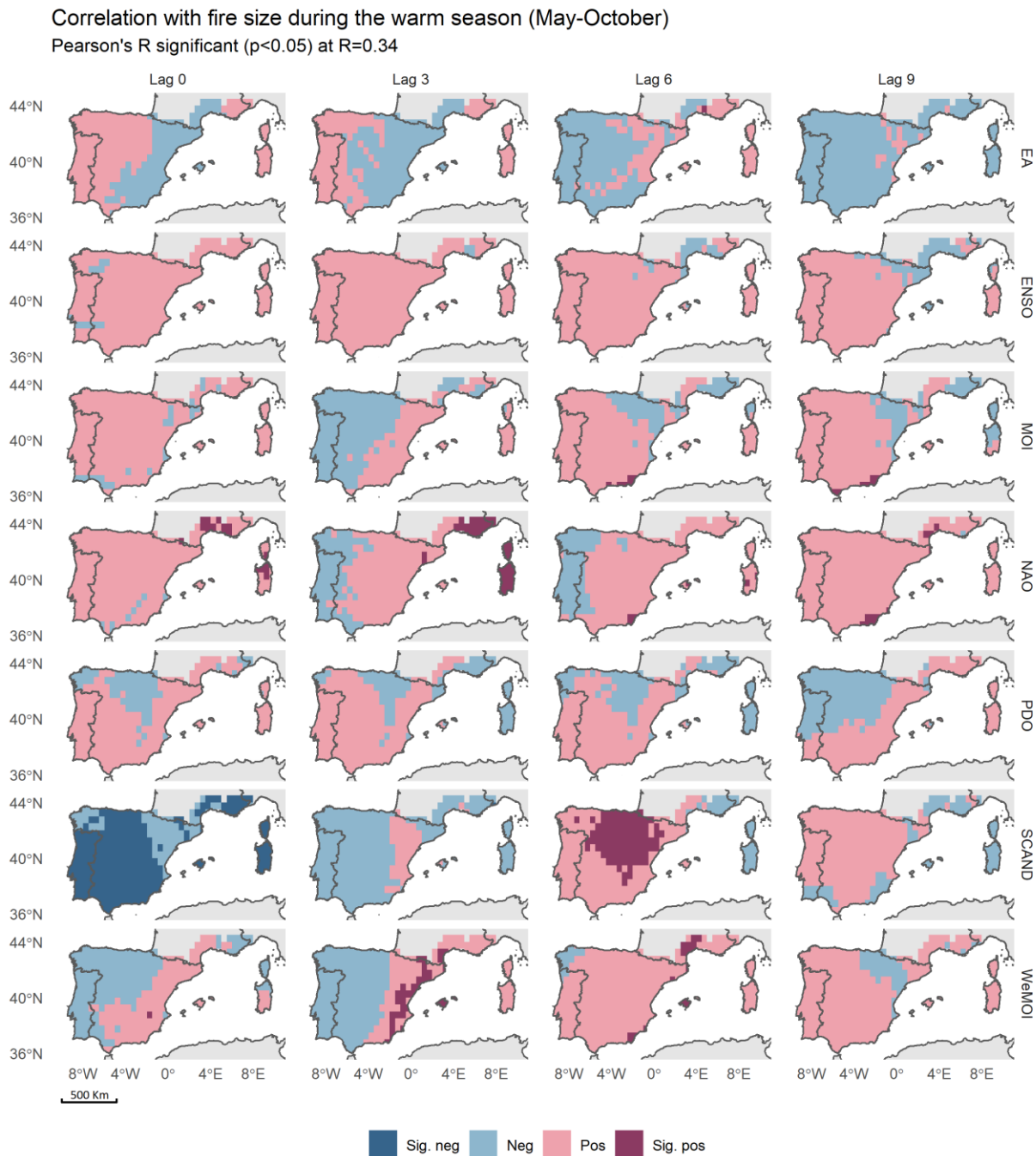
253  
 254 **Figure 1.** Spatial distribution of Pearson's R correlation coefficient between CTs and burned area  
 255 (fires > 100ha), 1980-2015. Columns indicate lagged cross-correlation intervals of months before  
 256 summer season.



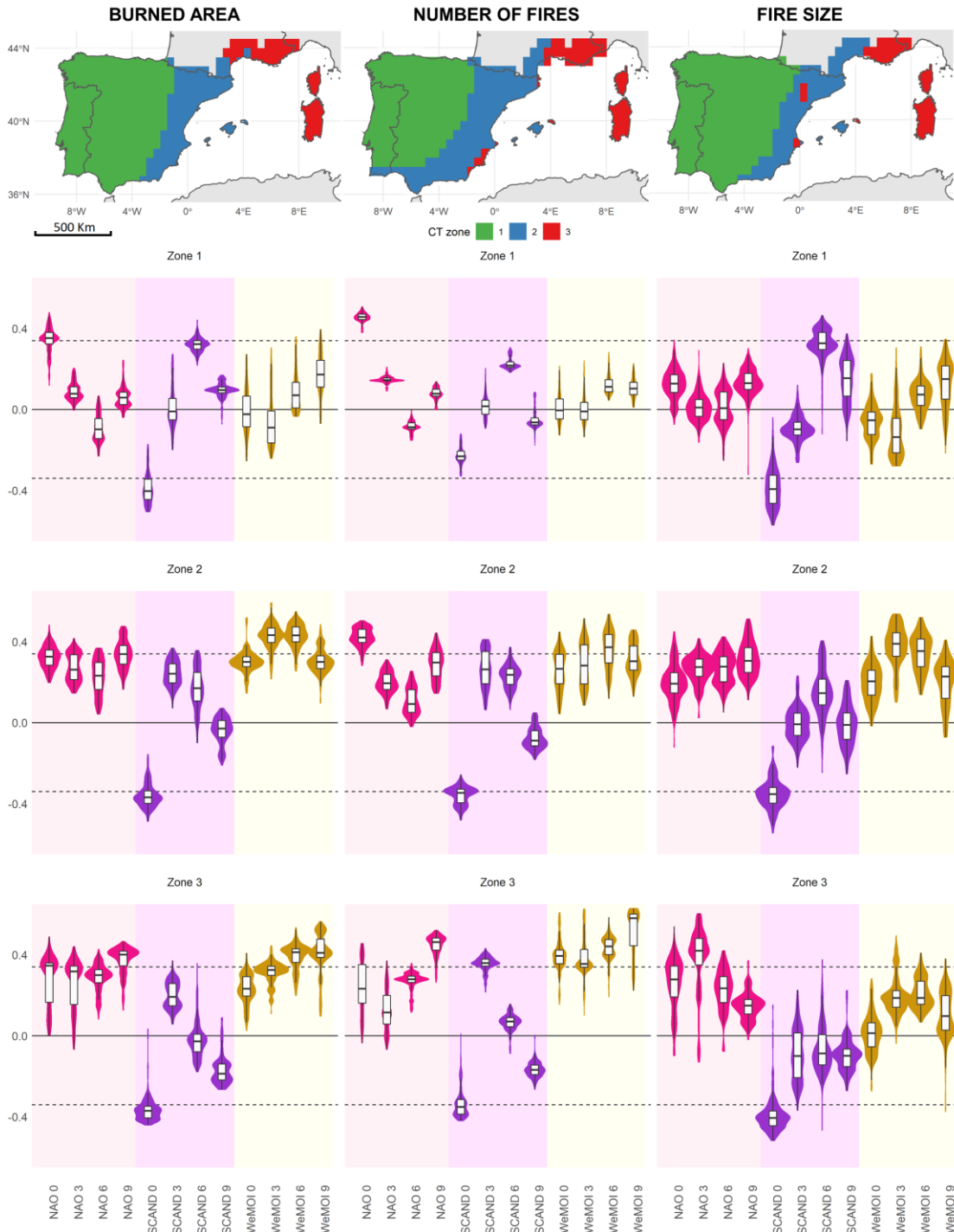
Correlation with number of fires during the warm season (May-October)  
 Pearson's R significant ( $p < 0.05$ ) at  $R = 0.34$



257  
 258 **Figure 2.** Spatial distribution of Pearson's R correlation coefficient between CTs and number of  
 259 fires (fires > 100ha), 1980-2015. Columns indicate lagged cross-correlation intervals of months  
 260 before summer season.  
 261  
 262  
 263



264  
 265 **Figure 3.** Spatial distribution of Pearson's R correlation coefficient between CTs and 95th  
 266 percentile of fire size (fires > 100ha), 1980-2015. Columns indicate lagged cross-correlation  
 267 intervals of months before summer season.



268

269 **Figure 4.** Climate teleconnection domains. Maps show the spatial distribution of CTs' domains  
 270 for burned area (left), number of fires (middle) and fire size (right). violin plots display the  
 271 correlation strength (Pearsons' R) between NAO, SCAND and WeMOi per feature and lag. The  
 272 solid black line indicates the 0 correlation threshold. Inner and outer dashed lines indicate the  
 273 significance threshold  $p < 0.05$ .

## 274 **5 Discussion and conclusions**

275 Several studies already prompt the importance of anticipating the pernicious effects of  
276 future shifts in fire regimes, with a wide consensus about the growing impacts of climate  
277 warming cascading into increased extreme wildfire events (Bedia et al., 2015, 2014; Ruffault et  
278 al., 2020; Turco et al., 2018). In this paper we provide insights into the dominant CT patterns  
279 modulating wildfire activity in the Western Mediterranean basin.

280 In line with Royé et al. (2020), we identified three CT domains spanning west-to-east and  
281 being mainly associated with the SCAND, the NAO and the WeMOi climate modes. From a  
282 spatial standpoint, the mediterranean coast CT domain (zone 2) largely matches fire regime  
283 zones delineated in the region (Rodrigues et al., 2020; Rodrigues et al., 2019a; Trigo et al., 2016)  
284 Vieira, Russo and Trigo, 2018). According to Calheiros, Pereira and Nunes (2021), this region is  
285 likely to persist over time and the frequency of days experiencing extreme fire-weather  
286 conditions will increase; an analysis that should consider the aforementioned CT modes  
287 influencing this domain in future analysis. Our domain delimitation assigns the rest of the IP into  
288 a single cluster (zone 1), despite the known variety of driving forces and different fire regimes  
289 (Nunes et al., 2016; Rodrigues et al., 2018). However, from a climate perspective, large fires in  
290 the region (>100 ha) seem to respond to similar spatial (Rodrigues et al., 2020) and temporal  
291 (Silva et al., 2019) patterns. The domains observed in France span from zone 3 in the East, to  
292 zone 2 in the west. They match to a certain degree the ‘pyroclimate’ delimitation by (Curt et al.,  
293 2014). However, the coarse spatial resolution of our fire data (50x50 km compared to the 2x2 km  
294 resolution of the French database) precluded us from detecting the fine-grained mosaic of local  
295 regions.

296 These CTs differently interacted across space and time (time lags between the CT and  
297 fire season), thus leading to different driving weather patterns described below. The negative  
298 relationship with the SCAND observed 0-3 months before summer involves reduced  
299 precipitation, suggesting drought spells influencing dead fuel moisture content as the main  
300 climate driver of wildfires (Ruffault et al., 2018). One of the most striking results was the  
301 observed phase transition of the SCAND (from positive to negative, i.e., wet to dry conditions)  
302 related to increased fire activity. This sharp shift suggests fuel build-up during +SCAND  
303 (increased rainfall) coupled to dry spells (-SCAND) fostering the accumulation of low dead fuel  
304 moisture content in the months leading up to summer. This indicates a certain limiting effect of  
305 dead biomass/fuel availability (herbaceous fuel load) in the ultimate dimensions of the burning  
306 (Gouveia et al., 2016; Littell et al., 2018) while supporting the notion that wildfires in the  
307 western Mediterranean are usually events fostered by short-term fire-prone conditions modulated  
308 by the moisture status and abundance of herbaceous dead fuels. This is in line also with the  
309 results of (Russo et al., 2017) for the IP, which highlight the relationship between wildfires and  
310 drought is better explained by the influence of spring precipitation on the central sector, and by  
311 the influence of temperature and precipitation during summer on most of the Portuguese  
312 provinces. Thus we should not overlook antecedent positive water balance anomalies  
313 (+SCAND), which may play an equally important role as dry spells or heat waves do (Pausas  
314 and Fernández-Muñoz, 2012; Pausas and Paula, 2012).

315 The NAO is linked to a higher number of fires in the entire region. Positive NAO is  
316 linked to anticyclonic conditions boosting temperature and limiting precipitation potentially  
317 leading to extreme drought episodes (García-Herrera et al., 2007; Vicente-serrano and Cuadrat,  
318 2007). Eventually, this situation may evolve into thermal lows and thunderstorms fostering

319 lightning strikes and fires (Pineda and Rigo, 2017). Likewise, NAO may connect also with sub  
320 saharan intrusions due to Atlantic blocking (Sousa et al., 2019, 2018), boosting temperatures in  
321 the Mediterranean area. In fact, the largest fires in the Mediterranean side of the IP seem to be  
322 associated with southeastern advections conducive to extreme heat waves (Rodrigues et al.,  
323 2020; Rodrigues et al., 2019b). Likewise, fires are known to be concomitant with thermal  
324 anomalies in the northeastern end of the IP (Cardil et al., 2015; Duane and Brotons, 2018) or  
325 Sardinia and Corsica (Ager et al., 2014; Salis et al., 2021). Though weaker than NAO's, the  
326 WeMOI also exerts moderate influence in the Mediterranean rim of the IP. During the +WeMOI  
327 the prevailing winds on the IP are typically from the West and Northwest. These winds, by the  
328 time they reach the Mediterranean sea, have crossed the peninsular continental areas reaching the  
329 leeward side of the coastal mountain systems, thus becoming warm and dry westerly winds  
330 (Rodrigues et al., 2019b) or cool but equally dry northwesterly winds (Duane and Brotons, 2018;  
331 Ruffault et al., 2017).

332 Nonetheless, while fires in the IP seem to be modulated by NAO, fire activity in southern  
333 France, Corsica and Sardinia (zone 3) is better associated with the WeMOI pattern. For instance,  
334 in the period 1998-2016, Sardinia presented the most relevant wildfire spread conditions in days  
335 with southern and southwestern winds. Slightly more than 50% of the area burned by very large  
336 wildfires (>200 ha) during these wind regimes (Salis et al., 2021). Moreover, the advection of  
337 hot and dry air masses from the south through the inner parts and the north end of the island  
338 resulted in an evident increasing gradient in wildfire size and risk from southern to inner and  
339 northern Sardinia. On the other hand, strong mistral winds from the west and north-west  
340 (dominant during the positive phase of the WeMOI) promoted an increase in wildfire size and  
341 area burned in eastern and southern zones of Sardinia (Salis et al., 2021).

342 By identifying the key CT patterns boosting wildfire activity and its spatial-temporal  
343 domains of influence we can leverage operational climate services to provide seasonal forecasts  
344 that can be used to complement early warning systems (Lledó et al., 2020). While early warning  
345 systems based on short-term forecasted weather conditions are useful to anticipate hazardous fire  
346 behavior and danger in operational environments, CTs modulate weather patterns at monthly  
347 scales with lagged effects as shown in this manuscript, facilitating the identification of adverse  
348 fire windows during the fire season. Furthermore, it is possible to produce long-term (up to 3-  
349 months) predictions of CT patterns (Świerczyńska-Chłaściak and Niedzielski, 2020; Wang et al.,  
350 2017) which can allow for some predictability and therefore contributing to the improvement of  
351 alert systems. Finally, the ultimate effects of CTs on key weather parameters influencing fire  
352 behavior such as fuel loading, dead and live fuel moisture content or wind fields should be  
353 further analyzed.

## 354 **Acknowledgments**

355 This work was partially supported by national funds through FCT (Fundação para a Ciência e a  
356 Tecnologia, Portugal) through projects IMPECAF (PTDC/CTA – CLI/28902/2017) and  
357 UIDB/50019/2020 - Instituto Dom Luiz.

## 358 **Data Availability Statement**

359 Data used in the study are available at Zenodo via DOI 10.5281/zenodo.5138095  
360 (<https://zenodo.org/record/5138095>) with Creative Commons Attribution 4.0 International  
361 license. Fire data were obtained from the following national/regional wildfire databases:

- 362 - Portugal (ICNF, <http://www2.icnf.pt/portal/florestas/dfci/inc/estat-sgif>)
- 363 - Spain (EGIF; [https://www.miteco.gob.es/es/biodiversidad/servicios/banco-datos-](https://www.miteco.gob.es/es/biodiversidad/servicios/banco-datos-naturaleza/informacion-disponible/incendios-forestales.aspx)  
364 [naturaleza/informacion-disponible/incendios-forestales.aspx](https://www.miteco.gob.es/es/biodiversidad/servicios/banco-datos-naturaleza/informacion-disponible/incendios-forestales.aspx))
- 365 - France (Prométhée; <https://www.promethee.com/incendies>)
- 366 - Sardinia (CFVA;  
367 [http://www.sardegnaeoportale.it/webgis2/sardegnamappe/?map=aree\\_tutellate](http://www.sardegnaeoportale.it/webgis2/sardegnamappe/?map=aree_tutellate)).

368 Data for climate teleconnection patterns were provided by the Climatic Research Unit from the  
369 University of East Anglia, the Climatology Group from the Universitat de Barcelona, and the  
370 US's Climate Prediction Center. Individual datasets and calculations can be accessed as follows:

- 371 - The NAO computed as the Gibraltar- Reykjavik normalized Sea Level Pressure (Jones,  
372 Jonsso and Wheeler, 1997); <https://crudata.uea.ac.uk/cru/data/nao/nao.dat>.
- 373 - The EA teleconnection pattern index, which is structurally similar to the NAO, and  
374 consists of a north-south dipole of anomaly centers spanning the North Atlantic from east to west  
375 (Barnston and Livezey, 1987). <http://www.cpc.ncep.noaa.gov/data/teledoc/ea.shtml>
- 376 - The SCAND, which consists of a primary circulation center over Scandinavia, with  
377 weaker centers of opposite sign over western Europe and eastern Russia/ western Mongolia, and  
378 known there as Eurasia-1 (Barnston and Livezey, 1987).  
379 <https://www.cpc.ncep.noaa.gov/data/teledoc/scand.shtml>
- 380 - The ENSO, which was calculated from the HadISST1. It is the area averaged sea surface  
381 temperature (SST) from 5S-5N and 170-120W (Rayner et al., 2003).  
382 [https://psl.noaa.gov/gcos\\_wgsp/Timeseries/Nino34/](https://psl.noaa.gov/gcos_wgsp/Timeseries/Nino34/)
- 383 - The PDO, which was derived as the leading PC of monthly SST anomalies in the North  
384 Pacific Ocean, poleward of 20N (Mantua et al., 1997).  
385 <https://psl.noaa.gov/data/climateindices/list/>
- 386 - The MOI, defined by Conte, Giuffrida and Tedesco (1989) as the normalized pressure  
387 difference between Algiers and Cairo; <https://crudata.uea.ac.uk/cru/data/moi/moi1.output.dat>.
- 388 - The WeMOi, which is an index measuring the difference between the standardized  
389 atmospheric pressure recorded at Padua in northern Italy, and San Fernando, Cádiz in  
390 Southwestern Spain (Martin-Vide and Lopez-Bustins, 2006);  
391 [http://www.ub.edu/gc/documents/Web\\_WeMOi-2020.txt](http://www.ub.edu/gc/documents/Web_WeMOi-2020.txt).

392 All analyses, maps and plots were conducted using the R's framework for statistical computing,  
393 Version 4.1.0, available via <https://cran.r-project.org/> (R Core Team, 2021).

## 394 **References**

- 395 Ager, A. A. et al. (2014) 'Wildfire risk estimation in the Mediterranean area', *Environmetrics*,  
396 25(6), pp. 384–396. doi: 10.1002/env.2269.

- 397 AghaKouchak, A. et al. (2020) ‘Climate Extremes and Compound Hazards in a Warming  
398 World’, *Annual Review of Earth and Planetary Sciences*, 48(1), pp. 519–548. doi:  
399 10.1146/annurev-earth-071719-055228.
- 400 Andela, N. et al. (2017) ‘A human-driven decline in global burned area’, *Science*, 356(6345), pp.  
401 1356–1361. doi: 10.1126/science.aal4108.
- 402 Ascoli, D. et al. (2017) ‘Inter-annual and decadal changes in teleconnections drive continental-  
403 scale synchronization of tree reproduction’, *Nature Communications*, 8(1), p. 2205. doi:  
404 10.1038/s41467-017-02348-9.
- 405 Barnston, A. G. and Livezey, R. E. (1987) ‘Classification, Seasonality and Persistence of Low-  
406 Frequency Atmospheric Circulation Patterns’, *Monthly Weather Review*, 115(6), pp.  
407 1083–1126. doi: 10.1175/1520-0493(1987)115<1083:CSAPOL>2.0.CO;2.
- 408 Bedia, J. et al. (2013) ‘Robust projections of Fire Weather Index in the Mediterranean using  
409 statistical downscaling’, *Climatic Change*, 120, pp. 229–247. doi: 10.1007/s10584-013-  
410 0787-3.
- 411 Bedia, J. et al. (2014) ‘Forest fire danger projections in the Mediterranean using ENSEMBLES  
412 regional climate change scenarios’, *Climatic Change*, 122(1–2), pp. 185–199. doi:  
413 10.1007/s10584-013-1005-z.
- 414 Bedia, J. et al. (2015) ‘Global patterns in the sensitivity of burned area to fire-weather:  
415 Implications for climate change’, *Agricultural and Forest Meteorology*, 214–215, pp.  
416 369–379. doi: 10.1016/J.AGRFORMET.2015.09.002.
- 417 Bond, W. J., Woodward, F. I. and Midgley, G. F. (2005) ‘The global distribution of ecosystems  
418 in a world without fire’, *New Phytologist*, 165(2), pp. 525–538. doi:  
419 <https://doi.org/10.1111/j.1469-8137.2004.01252.x>.
- 420 Bowman, D. M. J. S. et al. (2017) ‘Human exposure and sensitivity to globally extreme wildfire  
421 events’, *Nature Ecology & Evolution*, 1(3), p. 0058. doi: 10.1038/s41559-016-0058.
- 422 Bowman, D. M. J. S. et al. (2020) ‘Vegetation fires in the Anthropocene’, *Nature Reviews Earth  
423 & Environment*, 1(10), pp. 500–515. doi: 10.1038/s43017-020-0085-3.
- 424 Brönnimann, S. (2007) ‘Impact of el Niño–Southern Oscillation in European climate’, *Reviews  
425 of Geophysics*, 45, pp. 1–28. doi: 10.1029/2006RG000199.1.INTRODUCTION.
- 426 Brunner, L., Hegerl, G. C. and Steiner, A. K. (2017) ‘Connecting Atmospheric Blocking to  
427 European Temperature Extremes in Spring’, *Journal of Climate*, 30(2), pp. 585–594. doi:  
428 10.1175/JCLI-D-16-0518.1.
- 429 Cai, W. et al. (2014) ‘Increasing frequency of extreme El Niño events due to greenhouse  
430 warming’, *Nature Climate Change*, 4(2), pp. 111–116. doi: 10.1038/nclimate2100.

- 431 Calheiros, T., Pereira, M. G. and Nunes, J. P. (2021) ‘Assessing impacts of future climate change  
 432 on extreme fire weather and pyro-regions in Iberian Peninsula’, *Science of The Total*  
 433 *Environment*, 754, p. 142233. doi: <https://doi.org/10.1016/j.scitotenv.2020.142233>.
- 434 Camiá, A. et al. (2009) ‘Weather factors and fire danger in the Mediterranean’, in Chuvieco, E.  
 435 (ed.) *Earth Observation of Wildland Fires in Mediterranean Ecosystems*. Verlag:  
 436 Springer-Verlag, pp. 71–82.
- 437 Cardil, A. et al. (2021) ‘Coupled effects of climate teleconnections on drought, Santa Ana winds  
 438 and wildfires in southern California’, *Science of The Total Environment*, 765, p. 142788.  
 439 doi: <https://doi.org/10.1016/j.scitotenv.2020.142788>.
- 440 Cardil, A., Eastaugh, C. S. and Molina, D. M. (2015) ‘Extreme temperature conditions and  
 441 wildland fires in Spain’, *Theoretical and Applied Climatology*, 122(1–2), pp. 219–228.  
 442 doi: [10.1007/s00704-014-1295-8](https://doi.org/10.1007/s00704-014-1295-8).
- 443 Charrad, M. et al. (2014) ‘{NbClust}: An {R} Package for Determining the Relevant Number of  
 444 Clusters in a Data Set’, *Journal of Statistical Software*, 61(6), pp. 1–36.
- 445 Conte, M., Giuffrida, A. and Tedesco, S. (1989) *The Mediterranean Oscillation. Impact on*  
 446 *precipitation and hydrology in Italy* Climate Water. Helsinki: Publications of the  
 447 Academy of Finland.
- 448 Curt, T., Fréjaville, T. and Bouillon, C. (2014) ‘Characterizing pyroregions in south-eastern  
 449 France’, in *Characterizing pyroregions in south-eastern France*. Coimbra: Imprensa da  
 450 Universidade de Coimbra, pp. 1093–1101. doi: [10.14195/978-989-26-0884-6\\_119](https://doi.org/10.14195/978-989-26-0884-6_119).
- 451 Duane, A. and Brotons, L. (2018) ‘Synoptic weather conditions and changing fire regimes in a  
 452 Mediterranean environment’, *Agricultural and Forest Meteorology*, 253–254(February),  
 453 pp. 190–202. doi: [10.1016/j.agrformet.2018.02.014](https://doi.org/10.1016/j.agrformet.2018.02.014).
- 454 Dupuy, J. L. et al. (2020) ‘Climate change impact on future wildfire danger and activity in  
 455 southern Europe: a review’, *Annals of Forest Science*, 77(2). doi: [10.1007/s13595-020-](https://doi.org/10.1007/s13595-020-00933-5)  
 456 [00933-5](https://doi.org/10.1007/s13595-020-00933-5).
- 457 Fréjaville, T. and Curt, T. (2015) ‘Spatiotemporal patterns of changes in fire regime and climate:  
 458 defining the pyroclimates of south-eastern France (Mediterranean Basin)’, *Climatic*  
 459 *Change*, 129(1–2), pp. 239–251. doi: [10.1007/s10584-015-1332-3](https://doi.org/10.1007/s10584-015-1332-3).
- 460 Gallego, M. C., García, J. A. and Vaquero, J. M. (2005) ‘The NAO signal in daily rainfall series  
 461 over the Iberian Peninsula’, in.
- 462 Ganteaume, A. et al. (2013) ‘A Review of the Main Driving Factors of Forest Fire Ignition Over  
 463 Europe’, *Environmental Management*, 51(3), pp. 651–662. doi: [10.1007/s00267-012-](https://doi.org/10.1007/s00267-012-9961-z)  
 464 [9961-z](https://doi.org/10.1007/s00267-012-9961-z).



- 465 García-Herrera, R. et al. (2007) ‘The Outstanding 2004/05 Drought in the Iberian Peninsula:  
466 Associated Atmospheric Circulation’, *Journal of Hydrometeorology*, 8(3), pp. 483–498.  
467 doi: 10.1175/JHM578.1.
- 468 Gouveia, C. M. et al. (2016) ‘The outstanding synergy between drought, heatwaves and fuel on  
469 the 2007 Southern Greece exceptional fire season’, *Agricultural and Forest Meteorology*,  
470 218–219, pp. 135–145. doi: 10.1016/j.agrformet.2015.11.023.
- 471 Harris, S. and Lucas, C. (2019) ‘Understanding the variability of Australian fire weather between  
472 1973 and 2017’, *PLOS ONE*, 14(9), pp. 1–33. doi: 10.1371/journal.pone.0222328.
- 473 Hoerling, M. et al. (2012) ‘On the Increased Frequency of Mediterranean Drought’, *Journal of*  
474 *Climate*, 25(6), pp. 2146–2161. doi: 10.1175/JCLI-D-11-00296.1.
- 475 Jones, M. W. et al. (2019) ‘Global fire emissions buffered by the production of pyrogenic  
476 carbon’, *Nature Geoscience*, 12(9), pp. 742–747. doi: 10.1038/s41561-019-0403-x.
- 477 Jones, P. D., Jonsson, T. and Wheeler, D. (1997) ‘Extension to the North Atlantic oscillation  
478 using early instrumental pressure observations from Gibraltar and south-west Iceland’,  
479 *International Journal of Climatology*, 17(13), pp. 1433–1450. doi: 10.1002/(SICI)1097-  
480 0088(19971115)17:13<1433::AID-JOC203>3.0.CO;2-P.
- 481 Kitzberger, T. et al. (2007) ‘Contingent Pacific↔Atlantic Ocean  
482 influence on multicentury wildfire synchrony over western North America’, *Proceedings*  
483 *of the National Academy of Sciences*, 104(2), pp. 543–548. doi:  
484 10.1073/pnas.0606078104.
- 485 Koutsias, N. et al. (2013) On the relationships between forest fires and weather conditions in  
486 Greece from long-term national observations (1894–2010), *International Journal of*  
487 *Wildland Fire*. (4). Available at: <http://dx.doi.org/10.1071/WF12003>.
- 488 Koutsias, N. et al. (2016) ‘Fire occurrence zoning from local to global scale in the European  
489 Mediterranean basin: Implications for multi-scale fire management and policy’, *IForest*,  
490 9, pp. 195–204.
- 491 Lionello, P. (2012) *The Climate of the Mediterranean Region : From the past to the future.*  
492 Elsevier Science.
- 493 Littell, J. S. et al. (2018) ‘Climate Change and Future Wildfire in the Western United States: An  
494 Ecological Approach to Nonstationarity’, *Earth’s Future*, 6(8), pp. 1097–1111. doi:  
495 <https://doi.org/10.1029/2018EF000878>.
- 496 Lledó, L. et al. (2020) ‘Seasonal prediction of Euro-Atlantic teleconnections from multiple  
497 systems’, *Environmental Research Letters*, 15(7), p. 074009. doi: 10.1088/1748-  
498 9326/ab87d2.

- 499 Mantua, N. J. et al. (1997) ‘A Pacific Interdecadal Climate Oscillation with Impacts on Salmon  
500 Production\*’, *Bulletin of the American Meteorological Society*, 78(6), pp. 1069–1080.  
501 doi: 10.1175/1520-0477(1997)078<1069:APICOW>2.0.CO;2.
- 502 Mariani, M., Veblen, T. T. and Williamson, G. J. (2018) ‘Climate Change Amplifications of  
503 Climate-Fire Teleconnections in the Southern Climate Change Amplifications of  
504 Climate-Fire Teleconnections in the Southern Hemisphere’, *Geophysical Research  
505 Letters*, 45. doi: 10.1029/2018GL078294.
- 506 Martin-Vide, J. and Lopez-Bustins, J.-A. (2006) ‘The Western Mediterranean Oscillation and  
507 rainfall in the Iberian Peninsula’, *International Journal of Climatology*, 26(11), pp. 1455–  
508 1475. doi: 10.1002/joc.1388.
- 509 Modugno, S. et al. (2016) ‘Mapping regional patterns of large forest fires in Wildland–Urban  
510 Interface areas in Europe’, *Journal of Environmental Management*, 172(Supplement C),  
511 pp. 112–126. doi: <https://doi.org/10.1016/j.jenvman.2016.02.013>.
- 512 Moritz, M. A. et al. (2012) ‘Climate change and disruptions to global fire activity’, *Ecosphere*,  
513 3(6), p. art49. doi: <https://doi.org/10.1890/ES11-00345.1>.
- 514 Moritz, M. A. et al. (2014) ‘Learning to coexist with wildfire’, *Nature*, 515, p. 58.
- 515 Nunes, A. N., Lourenço, L. and Meira, A. C. C. (2016) ‘Exploring spatial patterns and drivers of  
516 forest fires in Portugal (1980–2014)’, *Science of The Total Environment*,  
517 573(Supplement C), pp. 1190–1202. doi: <https://doi.org/10.1016/j.scitotenv.2016.03.121>.
- 518 OrtizBevia, M. J. et al. (2016) ‘The multidecadal component of the {Mediterranean} summer  
519 variability’, *Clim Dyn*, 47(9–10), pp. 3373–3386. doi: 10.1007/s00382-016-3341-y.
- 520 Pausas, J. G. and Paula, S. (2012) ‘Fuel shapes the fire-climate relationship: evidence from  
521 Mediterranean ecosystems’, *Global Ecology and Biogeography*, 21(11), pp. 1074–1082.  
522 doi: 10.1111/j.1466-8238.2012.00769.x.
- 523 Pausas, JuliG. G. and Fernández-Muñoz, S. (2012) ‘Fire regime changes in the Western  
524 Mediterranean Basin: from fuel-limited to drought-driven fire regime’, *Climatic Change*,  
525 110(1–2), pp. 215–226. doi: 10.1007/s10584-011-0060-6.
- 526 Pereira, M. G. et al. (2011) ‘The history and characteristics of the 1980–2005 Portuguese rural  
527 fire database’, *Nat. Hazards Earth Syst. Sci.*, 11(12), pp. 3343–3358. doi: 10.5194/nhess-  
528 11-3343-2011.
- 529 Pineda, N. and Rigo, T. (2017) ‘The rainfall factor in lightning-ignited wildfires in Catalonia’,  
530 *Agricultural and Forest Meteorology*, 239, pp. 249–263. doi:  
531 <https://doi.org/10.1016/j.agrformet.2017.03.016>.
- 532 Power, S. et al. (2013) ‘Robust twenty-first-century projections of El Niño and related  
533 precipitation variability’, *Nature*, 502(7472), pp. 541–545. doi: 10.1038/nature12580.

- 534 R Core Team (2021). R: A language and environment for statistical computing. R Foundation for  
535 Statistical Computing, Vienna, Austria. URL <https://www.R-project.org/>.
- 536 Radeloff, V. C. et al. (2018) ‘Rapid growth of the US wildland-urban interface raises wildfire  
537 risk’, *Proceedings of the National Academy of Sciences*, 115(13), pp. 3314–3319. doi:  
538 10.1073/pnas.1718850115.
- 539 Rayner, N. A. et al. (2003) ‘Global analyses of sea surface temperature, sea ice, and night marine  
540 air temperature since the late nineteenth century’, *Journal of Geophysical Research:  
541 Atmospheres*, 108(D14). doi: 10.1029/2002JD002670.
- 542 Rodrigues, M. et al. (2018) ‘A comprehensive spatial-temporal analysis of driving factors of  
543 human-caused wildfires in Spain using Geographically Weighted Logistic Regression’,  
544 *Journal of Environmental Management*, 225, pp. 177–192. doi:  
545 <https://doi.org/10.1016/j.jenvman.2018.07.098>.
- 546 Rodrigues, M., González-Hidalgo, J. C., et al. (2019) ‘Identifying wildfire-prone atmospheric  
547 circulation weather types on mainland Spain’, *Agricultural and Forest Meteorology*, 264,  
548 pp. 92–103. doi: <https://doi.org/10.1016/j.agrformet.2018.10.005>.
- 549 Rodrigues, M., Costafreda-Aumedes, S., et al. (2019) ‘Spatial stratification of wildfire drivers  
550 towards enhanced definition of large-fire regime zoning and fire seasons’, *Science of The  
551 Total Environment*.
- 552 Rodrigues, M. et al. (2020) ‘Identifying large fire weather typologies in the Iberian Peninsula’,  
553 *Agricultural and Forest Meteorology*, 280. doi: 10.1016/j.agrformet.2019.107789.
- 554 Rodrigues, M. et al. (2021) ‘Do climate teleconnections modulate wildfire-prone conditions over  
555 the Iberian Peninsula?’, *Environmental Research Letters*. Available at:  
556 <http://iopscience.iop.org/article/10.1088/1748-9326/abe25d>.
- 557 Rodrigues, M., Jiménez-Ruano, A. and de la Riva, J. (2019) ‘Fire regime dynamics in mainland  
558 Spain. Part 1: Drivers of change’, *Science of The Total Environment*, p. 135841. doi:  
559 <https://doi.org/10.1016/j.scitotenv.2019.135841>.
- 560 Royé, D. et al. (2020) ‘Wildfire burnt area patterns and trends in Western Mediterranean Europe  
561 via the application of a concentration index’, *Land Degradation & Development*, 31(3),  
562 pp. 311–324. doi: <https://doi.org/10.1002/ldr.3450>.
- 563 Ruffault, J. et al. (2016) ‘Objective identification of multiple large fire climatologies: An  
564 application to a Mediterranean ecosystem’, *Environmental Research Letters*, 11(7). doi:  
565 10.1088/1748-9326/11/7/075006.
- 566 Ruffault, J. et al. (2017) ‘Daily synoptic conditions associated with large fire occurrence in  
567 Mediterranean France: evidence for a wind-driven fire regime’, *International Journal of  
568 Climatology*, 37(1), pp. 524–533. doi: 10.1002/joc.4680.

- 569 Ruffault, J. et al. (2018) 'Extreme wildfire events are linked to global-change-type droughts in  
570 the northern Mediterranean', *Natural Hazards and Earth System Sciences*, 18(3), pp. 847–  
571 856. doi: 10.5194/nhess-18-847-2018.
- 572 Ruffault, J. et al. (2020) 'Increased likelihood of heat-induced large wildfires in the  
573 Mediterranean Basin', *Scientific Reports*, 10(1), p. 13790. doi: 10.1038/s41598-020-  
574 70069-z.
- 575 Russo, A. et al. (2017) 'Assessing the role of drought events on wildfires in the Iberian  
576 Peninsula', *Agricultural and Forest Meteorology*, 237–238, pp. 50–59. doi:  
577 10.1016/j.agrformet.2017.01.021.
- 578 Salis, M. et al. (2021) 'Application of simulation modeling for wildfire exposure and  
579 transmission assessment in Sardinia, Italy', *International Journal of Disaster Risk  
580 Reduction*, 58, p. 102189. doi: <https://doi.org/10.1016/j.ijdr.2021.102189>.
- 581 Sánchez-Benítez, A. et al. (2018) 'June 2017: The Earliest European Summer Mega-heatwave of  
582 Reanalysis Period', *Geophysical Research Letters*, 45(4), pp. 1955–1962. doi:  
583 <https://doi.org/10.1002/2018GL077253>.
- 584 Silva, J. M. N. et al. (2019) 'Spatiotemporal trends of area burnt in the Iberian Peninsula, 1975–  
585 2013', *Regional Environmental Change*, 19(2), pp. 515–527. doi: 10.1007/s10113-018-  
586 1415-6.
- 587 Sousa, P. M. et al. (2011) 'Trends and extremes of drought indices throughout the 20th century  
588 in the Mediterranean', *Natural Hazards and Earth System Sciences*, 11(1), pp. 33–51. doi:  
589 10.5194/nhess-11-33-2011.
- 590 Sousa, P. M. et al. (2015) 'Different approaches to model future burnt area in the Iberian  
591 Peninsula', *Agricultural and Forest Meteorology*, 202, pp. 11–25. doi:  
592 10.1016/j.agrformet.2014.11.018.
- 593 Sousa, P. M. et al. (2018) 'European temperature responses to blocking and ridge regional  
594 patterns', *Climate Dynamics*, 50(1), pp. 457–477. doi: 10.1007/s00382-017-3620-2.
- 595 Sousa, P. M. et al. (2019) 'Saharan air intrusions as a relevant mechanism for Iberian heatwaves:  
596 The record breaking events of August 2018 and June 2019', *Weather and Climate  
597 Extremes*, 26, p. 100224. doi: <https://doi.org/10.1016/j.wace.2019.100224>.
- 598 Świerczyńska-Chłaściak, M. and Niedzielski, T. (2020) 'Forecasting the North Atlantic  
599 Oscillation index using altimetric sea level anomalies', *Acta Geodaetica et Geophysica*,  
600 55(4), pp. 531–553. doi: 10.1007/s40328-020-00313-5.
- 601 Trigo, R. M. et al. (2016) 'Modelling wildfire activity in Iberia with different atmospheric  
602 circulation weather types', *International Journal of Climatology*, 36(7), pp. 2761–2778.  
603 doi: 10.1002/joc.3749.

- 604 Turco, M. et al. (2013) ‘Impact of climate variability on summer fires in a Mediterranean  
605 environment (northeastern Iberian Peninsula)’, *Climatic Change*, 116(3–4), pp. 665–678.  
606 doi: 10.1007/s10584-012-0505-6.
- 607 Turco, M. et al. (2017) ‘On the key role of droughts in the dynamics of summer fires in  
608 Mediterranean Europe’, *Scientific Reports*, 7(1), p. 81. doi: 10.1038/s41598-017-00116-  
609 9.
- 610 Turco, M. et al. (2018) ‘Exacerbated fires in Mediterranean Europe due to anthropogenic  
611 warming projected with non-stationary climate-fire models’, *Nature Communications*,  
612 9(1), p. 3821. doi: 10.1038/s41467-018-06358-z.
- 613 Urbietta, I. R. et al. (2015) ‘Fire activity as a function of fire–weather seasonal severity and  
614 antecedent climate across spatial scales in southern Europe and Pacific western USA’,  
615 *Environmental Research Letters*, 10(11), p. 114013. doi: 10.1088/1748-  
616 9326/10/11/114013.
- 617 Vicente-serrano, S. M. and Cuadrat, J. M. (2007) ‘North Atlantic oscillation control of droughts’,  
618 pp. 357–358. doi: 10.1007/s10584-007-9285-9.
- 619 Vieira, I., Russo, A. and Trigo, R. M. (2020) ‘Identifying Local-Scale Weather Forcing  
620 Conditions Favorable to Generating Iberia’s Largest Fires’, *Forests*, 11(5). doi:  
621 10.3390/f11050547.
- 622 Vogel, J. et al. (2021) ‘Increasing compound warm spells and droughts in the Mediterranean  
623 Basin’, *Weather and Climate Extremes*, 32, p. 100312. doi: 10.1016/j.wace.2021.100312.
- 624 Wang, L., Ting, M. and Kushner, P. J. (2017) ‘A robust empirical seasonal prediction of winter  
625 NAO and surface climate’, *Scientific Reports*, 7(1), p. 279. doi: 10.1038/s41598-017-  
626 00353-y.
- 627 Zscheischler, J. et al. (2018) ‘Future climate risk from compound events’, *Nature Climate  
628 Change*, 8(6), pp. 469–477. doi: 10.1038/s41558-018-0156-3.
- 629  
630  
631